CONF-821072--1

INFLUENCE OF INJECTED HELIUM ON THE PHASE INSTABILITY OF ION-IRRADIATED STAINLESS STEEL*

E. A. Kenik and E. H. Lee
Metals and Ceramics Division, Oak Ridge National Laboratory

The influence of helium injection on phase instability under ion irradiation was studied for two modified 316 stainless steel alloys. Helium is required to nucleate voids in both alloys, though both exhibit phase instability without helium. The injected helium promotes associated growth of voids with precipitates. At low simultaneous helium injection rates (0–4 appm He/1 dpa), little or no effect on the precipitation process occurs. As the injection rate increases to 20 appm He/dpa, an increase in precipitate density and a decrease in precipitate size is observed. This result is in contrast to the observation that cold preinjected helium strongly suppresses the phase instability and swelling. The influence of helium on the phase instability is interpreted in terms of its effect on loop nucleation, which in turn influences the subsequent evolution of the damage microstructure.

*Research sponsored by the Division of Materials Sciences and the Office of Reactor Research and Technology, U.S. Department of Energy, under contract No. W-7405-eng-26 with the Union Carbide Corporation.

Introduction

Modified alloys of 316 stainless steel which exhibit good swelling resistance often also exhibit instability of the austenitic matrix under irradiation. The importance of helium and/or other gases in void nucleation is well recognized (1–3). However, the influence of helium on the evolution of the other components of the damage structure is not completely clear. Though there is a significant number of ion-irradiation studies which deal with the influence of helium on void swelling (4–11) and on dislocation structure (5,6,9–11), there are only a few which deal with the influence of helium on phase instability (9–11).

The present investigation deals with the influence of helium on the evolution of the damage structure and phase instability in two ion-irradiated, modified 316 stainless steel alloys, LS1A and LS1B. These alloys are silicon and titanium modified stainless steels developed at ORNL (4) which are highly swelling resistant under ion irradiation in the absence of helium, apparently as a result of a high barrier to void nucleation (11,12). In addition, both alloys exhibit solute segregation to dislocation loops (13) and marked phase instability of the austenitic matrix under ion irradiation (11–13).

Experimental

The LS1A alloy was arc-melted from high-purity constituents and the resulting chemistry is given in Table I. The LS1B alloy was a conventional, laboratory melt of similar composition. Specimens were 3-mm-diam disks punched from 0.75 mm sheet and final annealed at either 1050°C for 1 h (LS1A) or 1100°C for 15 min (LS1B). Disks were prepared on a vibratory polisher with various abrasives down to 0.1 μm diamond abrasive. Disks of LS1B were also given a final, brief electropolish on the mechanically polished surface. Irradiations were performed using 4 MeV Ni ions on the ORNL dual-beam Van de Graaff facility (14). Some specimens were simultaneously injected with helium at rates from 0.2–20 appm He/dpa. Other specimens were preinjected at 25°C to various helium levels and subsequently nickel ion irradiated. Others were injected at temperature partway through the irradiation. Bombardments were performed over the range 550–800°C at a dose rate of ~ 7×10^{-3} dpa/s. Disks were sectioned, back thinned to the peak damage depth (~0.7 μm) and examined using conventional transmission electron microscopy (CTEM) and analytical electron microscopy (AEM) on a JEM-120CX with energy dispersive spectroscopy (EDS) capability.

Table I. LS1A Alloy Composition

Weight Percent		Weight Percent	
Fe	64.6	Al	< 0.02
Cr	16.4	Nb	0.04
Ni	13.7	V	0.04
Mo	1.73	Co	< 0.005
Si	1.05	Zr	0.06
Mn	2.05	W	0.03
Ti	0.15	Cu	0.05

Results

Irradiations without Helium Injection

The evolution of the damage structures in uninjected LS1A and a nominal 316 stainless steel, G7, has been compared in a previous paper (11). Microstructural data for LS1A irradiated at 625°C are given for 1 dpa in Table II and for 10 and 70 dpa in Table III. At 1 dpa, 43-nm-diam Frank loops are present in uninjected LS1A at a density of ~ 3×10^{20} m^{-3} (24-nm-diam loops, 7×10^{20} m^{-3} for uninjected G7). At this dose level significant solute segregation of silicon and nickel to the dislocation loops is observed (13). Relative to G7, the dislocation loops in LS1A appear to unfault at a very low rate. Between 3 and 10 dpa, irradiation-induced precipitates replace the faulted loops; the loop density drops and a similar density of precipitates is observed; the average precipitate size is similar to that of the original loops; and an increase in the dislocation network density occurs (11). Two precipitate types occur — both are cubic phases with lattice parameters ~ 1.1 nm. One precipitate is tau phase (G phase), isostructural to $M_{23}C_6$. The second precipitate is eta phase (15) (H phase), isostructural to M_6C. Both phases are rich in silicon and nickel relative to the matrix. The degree of phase instability of the matrix increases with dose until saturating at ~5% precipitate volume fraction at ~70 dpa [Fig. 1(a)]. Estimated from precipitate chemistry and volume fraction, the matrix silicon concentration has been reduced to <60% of the original level at this dose. No void nucleation is observed in uninjected LS1A to dose levels ~600 dpa, where the swelling of a nominal 316 stainless steel (G7) is estimated as ~110%.

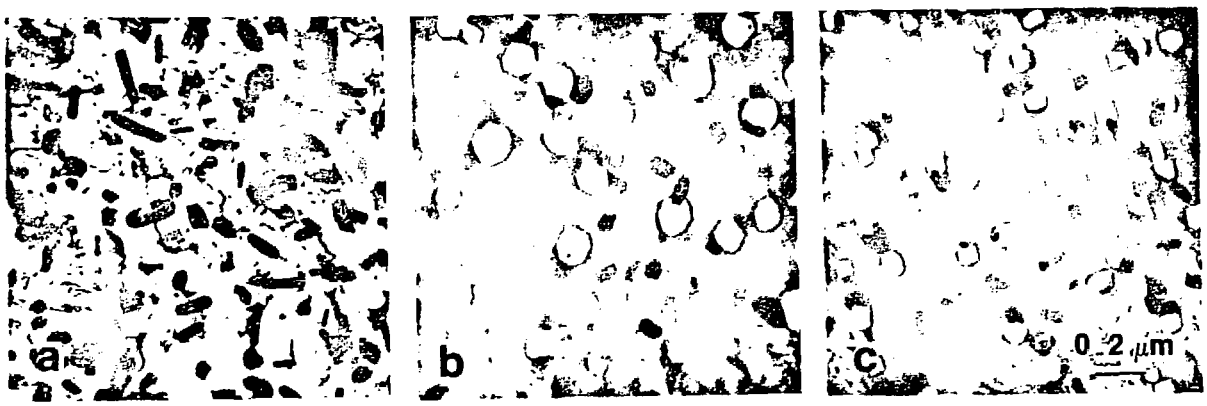

Fig. 1. Damage microstructure of LS1A irradiated to 70 dpa at 625°C. (a) Uninjected, (b,c) simultaneous helium injection, (b) 0.2 appm He/dpa, (c) 20 appm He/dpa.

Table II. Low Dose Microstructural Data for LS1A at 625°C

	1 dpa	
	$\bar{d}_L$ (nm)	N_L (m^{-3})
LS1A (Uninjected)	430	3×10^{20}
LS1A (Simultaneous) (0.2 appm He/dpa)	420	2×10^{20}
LS1A (20 appm He/dpa)	400	3×10^{20}
LS1A (Preinjected) (14 appm He)	<90	$>2 \times 10^{21}$

Table III. High Dose Microstructural Data for LS1A at 625°C

	10 dpa			70 dpa			
	$\bar{d}_v$ (nm)	N_v (m^{-3})	Swelling (%)	Λ (m/m^3)	$\bar{d}_v$ (nm)	N_v (m^{-3})	Swelling (%)
LS1A (Uninjected)		No voids		2.5×10^{14}		No voids	
LS1A (Simultaneous) (0.2 appm He/dpa)	35.0	5.9×10^{18}	0.015	4.1×10^{14}	71.0	1.5×10^{20}	3.5
LS1A (20 appm He/dpa)	20.0	6.4×10^{19}	0.036	3.6×10^{14}	43.0	3.6×10^{20}	1.8
LS1A (Preinjected) (14 appm He)		No voids		8.4×10^{13}	~10.0	$<2 \times 10^{19}$	$<1 \times 10^{-4}$
LS1A (Injected at 10 dpa)(14 appm He)		No voids		2.6×10^{14}	60.0	1.2×10^{20}	1.6

Figure 2 illustrates the damage microstructure of LS1B irradiated to 100 dpa over the temperature range 550–725°C without injected helium. As for LS1A, uninjected LS1B exhibits extensive phase instability under irradiation (forming both tau and eta phases) and a high resistance to void nucleation. As a function of irradiation temperature, the precipitate density decreases continuously, while precipitate size increases up to at least 700°C. The precipitate volume fraction reaches a maximum value of ~6% at ~700°C. A similar trend as a function of temperature is observed for the phase instability of LS1A.

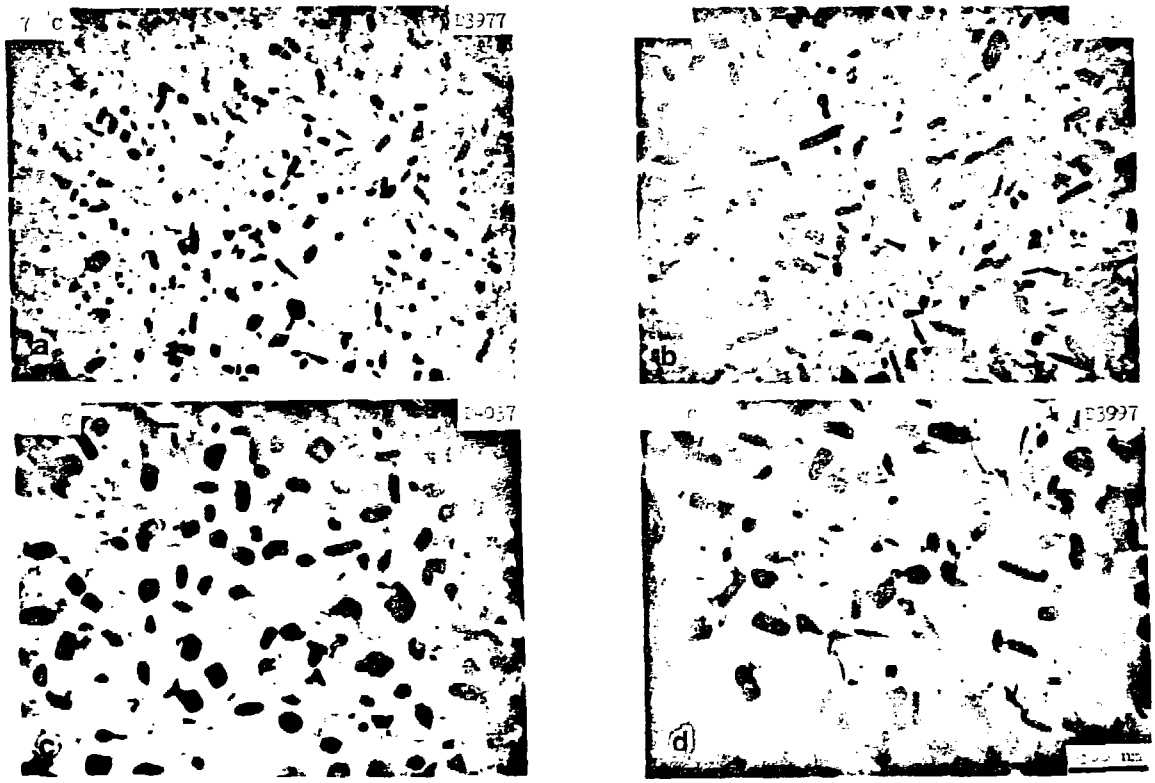

Fig. 2. Damage microstructure of uninjected LS1B irradiated to 100 dpa as a function of temperature. (a) 575°C, (b) 625°C, (c) 675°C, and (d) 725°C.

Simultaneous Helium Irradiations

With the simultaneous injection of helium during irradiation, significant changes occur in the higher dose (10–70 dpa) damage microstructures of LS1A (Fig. 1), while little change in the interstitial clustering in dislocation loops occurs at low doses (~1 dpa). Quantitative microstructural parameters are presented in Tables II and III. The dislocation loop density at 1 dpa and 625°C is essentially constant with respect to the rate of simultaneous helium injection, while the data indicate a slight decrease in average loop diameter. As in the uninjected case, the helium-injected LS1A exhibits precipitation by 10 dpa. However, in contrast to the uninjected case, at both helium injection rates, voids are observed, always in association with the radiation-induced precipitates. The inverse is not true in general, as not all precipitates have associated voids. At 70 dpa, 625°C (Fig. 1), the void densities and sizes increase for both injection rates, but the voids are still associated with the precipitates. While the hundredfold increase in helium more than doubles the void density, the void swelling is roughly halved as a result of the decreased void size. Assessing the degree of phase instability for these three irradiation conditions is difficult as a result of the precipitate-void association. It appears that the precipitate sizes decrease, while their number densities increase slightly in going from uninjected to 0.2 appm He/dpa irradiation and finally to 20 appm He/dpa. The general impression from Fig. 1 is that the degree of phase instability decreases with increasing amounts of simultaneously injected helium.

Figure 3 illustrates the influence of simultaneous helium injection on the damage structure of both solution-annealed and cold-worked LS1B after irradiation to 70 dpa at 675°C (the inset is a 3× enlargement). It should be noted that cold work decreases the amount of radiation-induced precipitation. Simultaneous helium injection results in formation of large voids in association with the precipitates. In addition, there is a second population of small cavities (~10 nm in diameter) which are probably gas bubbles. Increasing the helium injection rate increases the density of both populations. While there is little change in the precipitate microstructure between 0.4 and 4 appm He/dpa injection cases, there is significant refinement of scale in the precipitation for the 20 appm He/dpa irradiation. Precipitation density has been increased, while precipitate size has decreased. Very low swelling is exhibited for all helium injection rates in the irradiation of cold-worked LS1B, where phase instability is suppressed. Only in areas in which the cold work had undergone significant recovery was significant phase instability or swelling observed.

Preinjected Helium Irradiations

Room-temperature preinjection of helium at levels from 14 to 112 appm He results in significant modification of the damage structure evolution at both low and high dose levels (Tables II and III). In LS1A preinjected with 14 appm He, the loop structure at 1 dpa and 625°C is refined in scale; the loops are smaller in size (<90 nm in diameter), but are present in higher number densities relative to the uninjected or simultaneously injected cases. At 10 dpa, the damage structure is still comprised primarily of small dislocation loops. No phase instability or void formation is observed. The damage structure at 70 dpa was essentially the same as that at 10 dpa [Fig. [Fig. 4(a)]. However, a low density of ~10-nm-diam cavities was observed; the resultant swelling could only be estimated as $< 1 \times 10^{-4}\%$. As the preinjected helium level was increased sequentially up to 112 appm, the dislocation loop structure at 70 dpa remained constant, while the cavity density increased roughly tenfold. At helium levels <50 appm He, cavities ~17 nm in diameter appear in bands parallel to some grain boundaries [Fig. 4(a) inset] and the grain boundaries themselves contain high densities

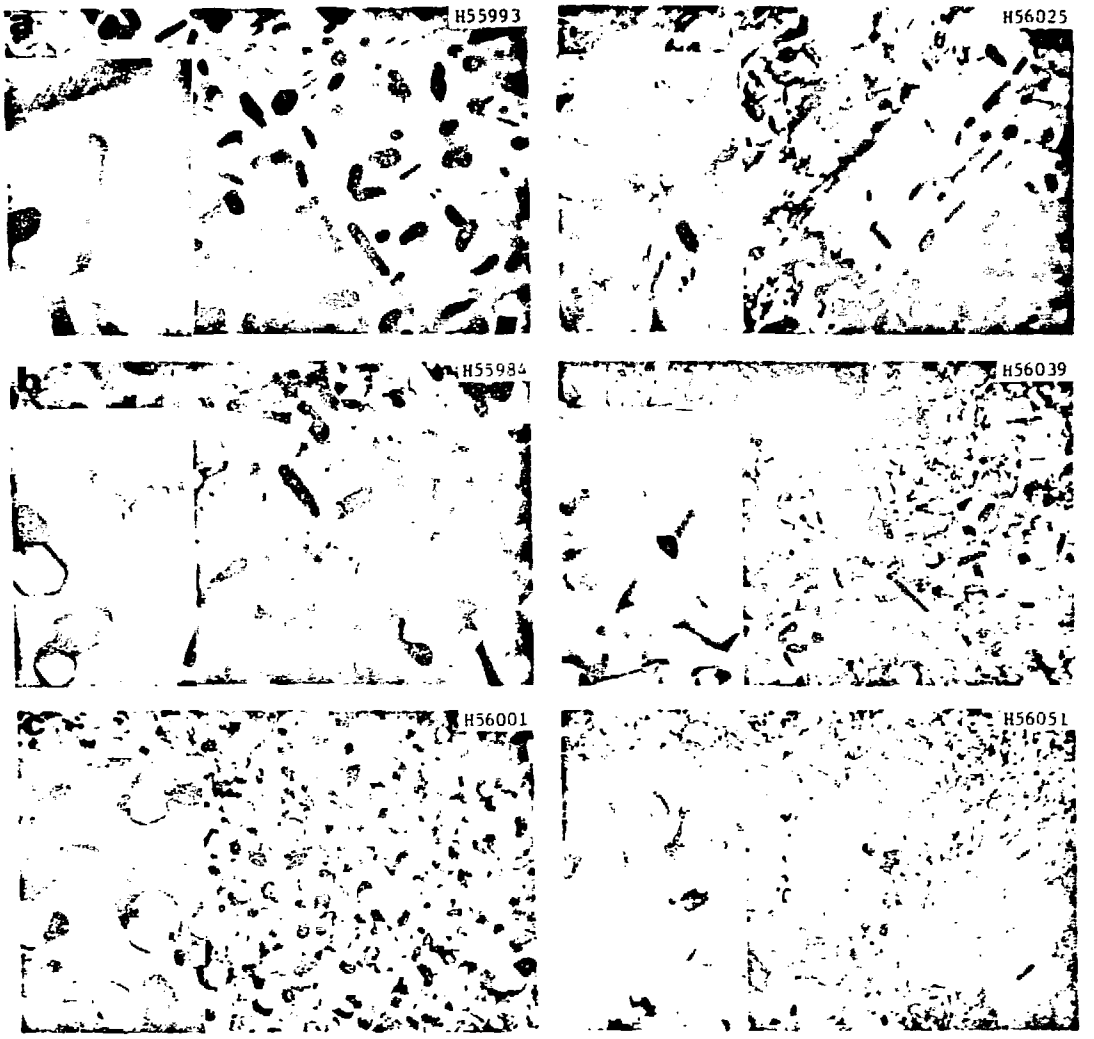

Fig. 3. Damage microstructure of solution-annealed (left) and cold-worked (right) LS1B irradiated to 70 dpa at 625°C with simultaneous helium injection at (a) 0.4 appm He/dpa, (b) 4 appm He/ dpa, (c) 20 appm He/dpa (inset is a 3× enlargement).

Fig. 4. Damage microstructure of LS1A irradiated to 70 dpa at 625°C. (a) 56 appm He cold preinjected, (b) 14 appm He injected at 10 dpa while at temperature.

of small cavities (~3 nm). For all helium preinjected irradiations, LS1A exhibited no phase instability of the matrix.

Two other experiments were performed to aid the understanding of the different effects of helium on the damage microstructural evolution. After irradiation to 10 dpa at 625°C, where loop nucleation is over and significant phase instability had occurred, 14 appm He was injected into LS1A at temperature and the irradiation was continued to 70 dpa. The resultant damage structure [Fig. 4(b)] was similar to that observed for simultaneous helium injection [Fig. 1(b,c)]. Quantitative data are summarized in Table III. In the second experiment, 400 appm He was injected at temperature into LS1B after a 70 dpa irradiation at 675°C. Cavity formation was observed at both irradiation-induced precipitates [best seen in Fig. 5(a) for solution annealed LS1B] and at dislocations [best seen in Fig. 5(b) for cold-worked LS1B].

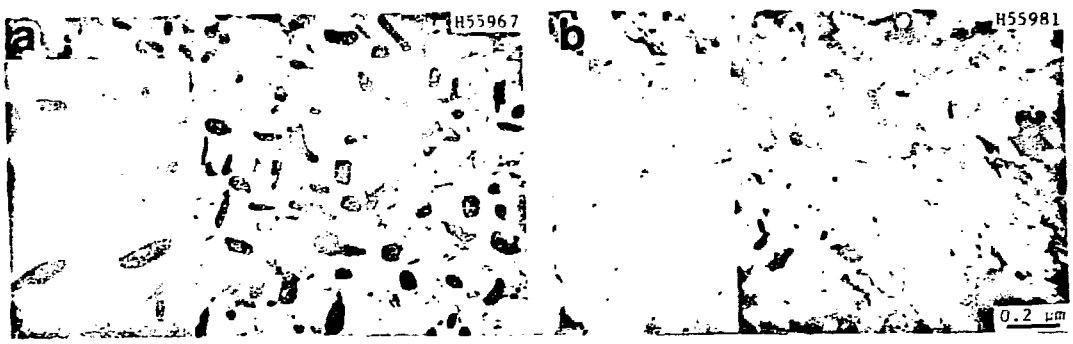

Fig. 5. Damage microstructure of LS1B irradiated to 70 dpa at 675°C, then injected with 400 appm He at temperature. (a) Solution annealed LS1B, (b) cold-worked LS1B (inset is a 3× enlargement).

Discussion

The response of the two alloys irradiated in the present study is representative of a wide range of both 316 stainless steel based alloys and other austenitic alloys in several ways. While the alloys exhibit good resistance to void swelling, which in many cases arises from difficult void nucleation, they do exhibit phase instability of the matrix under irradiation. In cases where void formation occurs, there is an association of the voids with the irradiation-induced precipitates. This association is often taken as evidence of a direct cause-and-effect relation between phase instability and swelling. However, irradiation of LS1A and LS1B without helium resulted in extensive phase instability without void formation. In addition, at low helium injection rates, it is observed that at low doses most irradiation-induced precipitates do not have associated voids. As irradiation continues additional voids are nucleated on the existing precipitates. Thus, while phase instability of these alloys may be a necessary condition for void swelling, it is not sufficient.

In many of the modified austenitic alloys which exhibit good swelling resistance, the phase instability observed is often preceded by segregation of solute elements under irradiation (13). In addition, the phases are often highly enriched in undersized solute elements, such as silicon and nickel. This is the case for irradiation-induced eta (H) phase (10,16,17), tau phase (G) (18,19), γ' (Ni_3Si) (20), and others. A proposed sequence of events involved in phase instability under irradiation has been outlined (11). Under the influence of the vacancy and/or interstitial fluxes, silicon

and nickel segregate to faulted dislocation loops (13). Their concentrations increase until one or both exceed some "solubility limit," (12) and an irradiation-induced second phase precipitates at the dislocation loop or its planar fault. Further solute segregation may occur as a result of defect fluxes to the precipitate interface, allowing further phase instability and solute depletion of the matrix. The suppression of phase instability by cold-work and appearance of precipitation in recovered regions of cold-worked material can both be explained by such a mechanism for irradiation-induced phase instability. The high dislocation density introduced by cold work modifies the segregation process in two ways. The high dislocation sink strength strongly suppresses the nucleation of faulted loops, removing in part the proposed site of localized solute segregation. Secondly, the dislocation network presents more than ten times larger dislocation line length than a loop structure for solute segregation. This increase will produce a decrease in the point defect fluxes to a given line segment, thus decreasing the maximum amount of solute segregation possible. In addition, the network dislocations glide and climb away from their original position under irradiation, leaving the segregated atoms behind. The faulted loops are restricted to movement by climb and cannot glide away from the segregation. As a cold-work structure recovers, the dislocation density decreases and the suppression of both loop nucleation and solute segregation decreases. In this fashion phase instability in cold-worked materials should be localized to recovered regions of the structure.

The results of the postirradiation injection of helium into LS1B indicate a strong attraction of helium to both dislocations and precipitates. Such an interaction of helium with defects could be reflected in changes in the evolution of damage microstructures during irradiations where helium is present. It is evident that the presence of helium is a prerequisite for void formation in both LS1A and LS1B during ion irradiation. This resistance to void nucleation in the absence of helium is attributable to the gettering of chemical interstitials (i.e., oxygen, nitrogen, etc.) by titanium and/or silicon (11). The gases would aid void nucleation by stabilizing the subcritical void nuclei. Helium provides an inert gas species to stabilize the voids in the modified alloys studied.

The influence of injected helium on the damage microstructural evolution appears to depend strongly on the amounts of helium present at one critical period in the microstructural development, the nucleation of the dislocation substructure. The different effects observed for the various modes of helium injection will be discussed in terms of this mechanism. In the case of preinjection, helium increases the number of dislocation loops at low doses, decreases their size, and extends the dose interval over which loops are observed. This refinement of the loop microstructure was exhibited for preinjected irradiations of both LS1A and a nominal 316 stainless steel, G7 (11). There are two possible mechanisms by which the preinjected helium could produce this effect — one arising from an interaction between the helium and interstitials (11), the other arising from an interaction between the helium and vacancies. On the basis of cluster calculations which indicate strong binding of helium to both vacancies and interstitials (21), the results of Johnson (22) would predict enhanced interstitial cluster nucleation during the transient period early in an irradiation. In this way, helium could influence the dislocation loop evolution. However, the survival of this high density of dislocation loops into the steady-state regime would depend on the behavior of the excess vacancies left by the interstitial clustering. The survival rate of these early interstitial clusters is the origin of the second mechanism by which helium influences the loop nucleation rate. It is proposed that the number of interstitial clusters nucleated during the transient period far exceeds

that of the dislocation loops which are observed in the steady-state regime. The loss of a part of the interstitial clusters arises from the partial annihilation of the excess vacancies at these clusters. The degree of annihilation of the clusters depends on the remainder of the sink structure. If no biased sinks (besides the clusters) are present, the interstitial clusters must eventually be annihilated completely. The continued evolution of the loop structure observed under irradiation indicates that some of the excess vacancies normally go to sinks other than the interstitial clusters. In the case of preinjected helium, it is proposed that the helium immobilizes some of the excess vacancies in clusters, thus increasing the survival rate of the interstitial clusters.

Either or both of these mechanisms could be operating to produce the high loop densities observed in preinjected materials. The subsequent competition between the larger number of loops for the irradiation-produced defects would reduce the defect fluxes to each of the dislocation loops, resulting in both lower growth rates and solute segregation rates. The smaller loop sizes would delay loop unfaulting and interaction to form a dislocation network. Such an effect explains both the observed refinement in scale of the loop substructure in preinjected LS1A and the survival of significant loop populations in such material to ~70 dpa; whereas loops disappear between 3 and 10 dpa in uninjected material. In addition, the reduced solute fluxes to each of the dislocation loops would suppress the phase instability. In this fashion, the effects of cold work and preinjected helium on phase instability are similar as they both provide increased number of sinks for solute segregation, reducing solute fluxes and suppressing phase instability.

The effects of simultaneous helium injection on the damage microstructural evolution are less pronounced, which is in agreement with the smaller amounts of helium present during the proposed critical period of dislocation loop nucleation. Only slight changes in microstructure occur at low helium injection rates for both LS1A and LS1B. At the high rates of injection the effects become more pronounced. In LS1A, there is a slight increase in loop density and slight decrease in loop size at 20 appm He/dpa. Similar increases in number density and decreases in size are observed for the precipitates after 70 dpa irradiations of LS1A and LS1B with 20 appm He/dpa injection. These observations are consistent with the proposed helium effects mechanism as follows. As sufficient helium becomes present during the loop nucleation step, more and smaller loops are formed as in the preinjected case. The effects are not as pronounced in the simultaneous injection case as the helium levels for that case are not as high (loop nucleation occurring well below 1 dpa). The loop nucleation (or survival) period may also be extended by the simultaneous helium injection relative to the uninjected case. These moderate changes in loop structure result in the observed increase in precipitate density and decrease in precipitate size.

The influence of helium on the void swelling of these alloys arises from two effects. If present in sufficient quantity during the loop nucleation process, the helium can influence the formation of the irradiation-induced precipitates which are the void formation sites. Simultaneous helium injection at rates approaching 20 appm He/dpa increases the precipitate density and supplies increased helium levels, both of which will promote increased void nucleation as observed. The resultant effect on void size and swelling is dependent on whether dislocations or voids are the dominant sinks for defects. In comparing the 0.2 and 20 appm He/dpa irradiations, the decrease in void size and swelling which occurred at 70 dpa indicates that the void growth kinetics may be void controlled for the 20 appm He/dpa case (11). It is possible that the association of voids and precipitates

effectively increases the void sink strength by the collection of point defects for the void at the precipitate-matrix interface as well as the void-matrix interface. Preinjected helium strongly curtails the phase instability of the alloys, removing the heterogeneous nucleation sites for voids. The cavities observed in this material at high doses appear to have grown as gas-driven bubbles. The same is probably true of the small cavities of the bimodal cavity distribution in the simultaneously injected LS1B.

The similarity of damage microstructure between simultaneous helium injected irradiations [Fig. 1(b,c)] and that of material injected at 10 dpa (where dislocation loop nucleation is completed and phase instability has initiated)[Fig. 4(b)] appears to indicate that helium has little or no effect on microstructural evolution after loop nucleation, except to aid in the void nucleation process. The association of voids with irradiation-induced precipitates in both alloys under simultaneous helium injected irradiation arises from either favorable void nucleation or growth at the precipitates. As the observed microstructural evolution indicates that the precipitates precede the voids, it is quite possible for several mechanisms to enhance the void nucleation rate at the precipitate interfaces. The precipitate can act as "collector" of point defects and/or helium giving an associated void nucleus an effective capture radius significantly larger than that of an isolated void nucleus. Both species would promote void nucleation preferentially at the interfaces of irradiation-induced precipitates which are not strong interstitial sinks. A similar precipitate "collector" effect has been shown to substantially enhance the growth of voids associated with such precipitates with respect to those isolated in the matrix (24).

Conclusions

1. Helium will modify dislocation substructure evolution if present in sufficient quantity during the loop nucleation period. This effect originates from helium enhancing either the nucleation or survival of interstitial clusters.

2. The primary role of helium with regard to phase instability arises from its influence on loop evolution. Increased loop nucleation results in increased number of solute segregation sites which form precipitates. Competition between these increased sites for the fixed amount of solute reduces the degree of phase instability. Helium preinjection is the extreme case where insufficient solute segregation occurs for phase instability to develop.

3. These alloys, which exhibit good swelling resistance under irradiation, also exhibit phase instability. The trapping of point defects to suppress swelling probably also results in solute segregation, which can lead to phase instability.

4. Cold work will suppress phase instability and swelling in these alloys. This effect has been attributed to the suppression of loop nucleation by the cold-work dislocation structure and the dilution of the segregating atoms to a larger sink density.

5. Helium has positive interactions with both dislocations and precipitates.

Acknowledgments

The authors wish to thank J. T. Houston and C. G. McKamey for specimen preparation, R. A. Buhl and M. B. Lewis for assistance with the ion irradiations, and L. K. Mansur and K. Farrell for excellent discussions.

References

1. K. Farrell, A. Wolfenden, and R. T. King, Rad. Effects 8, 107 (1971).
2. H. Wiedersich, J. J. Burton, and J. Katz, J. Nucl. Mater. 51, 287 (1974).
3. B.T.M. Loh, Acta Met. 20, 1305 (1972).
4. E. E. Bloom, J. O. Stiegler, A. F. Rowcliffe, and J. M. Leitnaker, Scripta Met. 10, 303 (1976).
5. N. H. Packan, K. Farrell, and J. O. Stiegler, J. Nucl. Mater. 78, 143 (1978).
6. J. L. Brimhall and E. P. Simonen, J. Nucl. Mater. 68, 235 (1977).
7. R. S. Nelson, P. J. Mazey, and J. A. Hudson, Voids Form by Irradiation of Reactor Materials, eds., S. F. Pugh, M. H. Loretto, and D.I.R. Norris, (BNS, Harwell), 1971, p. 191.
8. R. S. Nelson and J. A. Hudson, J. Nucl. Mater. 58, 11 (1975).
9. W. J. Choyke, J. N. McGruer, J. R. Townsend, J. A. Spitznagel, N. J. Doyle, and F. J. Venskytis, J. Nucl. Mater. 85&86, 647 (1979).
10. N. H. Packan and K. Farrell, ibid., p. 677.
11. E. A. Kenik, ibid., p. 659.
12. E. H. Lee, A. F. Rowcliffe, and E. A. Kenik, J. Nucl. Mater. 83, 79 (1979).
13. E. A. Kenik, Scripta Met. 10, 733 (1976).
14. M. B. Lewis, N. H. Packan, G. F. Wells, and R. A. Buhl, Nucl. Instr. & Methods 167, 233 (1979).
15. P. J. Maziasz, Scripta Met. 13, 621 (1979).
16. E. A. Kenik, Trans. ANS 27, 275 (1977).
17. T. M. Williams and J. M. Titchmarsh, J. Nucl. Mater. 87, 398 (1979).
18. L. E. Thomas, Trans. ANS 28, 151 (1978).
19. T. M. Williams, J. M. Titchmarsh, and D. R. Arkell, J. Nucl. Mater. 82, 199 (1979).
20. H. R. Brager and F. A. Garner, ASTM 9th International Symposium on Effects of Radiation on Structural Materials, STP-683 (1979), p. 207.
21. M. I. Baskes, C. L. Bisson, and W. D. Wilson, J. Nucl. Mater. 83, 139 (1979).
22. R. A. Johnson, ibid., p. 147.
23. L. K. Mansur, Nucl. Technol. 40(1), 5 (1978).
24. L. K. Mansur, to be published.